

## $Q^2$ dependence of diffractive vector meson electroproduction

A.D. Martin<sup>a</sup>, M.G. Ryskin<sup>a,b</sup> and T. Teubner<sup>c</sup>

<sup>a</sup> Department of Physics, University of Durham, Durham, DH1 3LE, England

<sup>b</sup> Petersburg Nuclear Physics Institute, Gatchina, St. Petersburg, 188350, Russia

<sup>c</sup> Institut für Theoretische Physik E, RWTH Aachen, D-52056 Aachen, Germany

### Abstract

We give a general formula for the cross section for diffractive vector meson electroproduction,  $\gamma^* p \rightarrow V p$ . We first calculate diffractive  $q\bar{q}$  production, and then use parton-hadron duality by projecting out the  $J^P = 1^-$  state in the appropriate mass interval. We compare the  $Q^2$  dependence of the cross section for the diffractive production of  $\rho$  and  $J/\psi$  mesons with recent HERA data. We include the characteristic  $Q^2$  dependence associated with the use of the skewed gluon distribution. We give predictions for  $\sigma_L/\sigma_T$  for both  $\rho$  and  $J/\psi$  production.

The diffractive leptonproduction of vector mesons at high energy is an interesting and important process. Indeed diffractive  $\gamma^*p \rightarrow Vp$  data, with  $V = \rho, \omega, \phi, J/\psi$  and  $\Upsilon$ , are becoming available with increasing precision from the experiments at HERA [1]–[9]. They offer the opportunity to study the vacuum-exchange singularity as a function of the virtuality  $Q^2$  of the incoming photon and of the mass  $M$  of the produced vector meson. Moreover observation of the vector meson decays allows both  $\sigma_L$  and  $\sigma_T$  to be measured, and even  $s$ -channel helicity conservation to be checked [4, 5, 8, 9].

Let us first review the description of diffractive electroproduction of  $\rho$  mesons; a process which has attracted a lot of theoretical interest [10]–[13]. At first, phenomenological parametrizations based on the vector-meson-dominance model and Regge exchanges were used. Then a non-perturbative two-gluon exchange model of the Pomeron was introduced [10]. For large  $Q^2$  however, we would expect that a pure perturbative QCD description is applicable. Such a description for the production of longitudinally polarised  $\rho$  mesons was given by Brodsky et al. [11], using the leading twist wave function for the  $\rho$  meson. The process is sketched in Fig. 1. However for the production of transversely polarized  $\rho$  mesons, the perturbative QCD approach encounters an infrared divergence in the integration over the quark transverse momentum. This problem can be overcome by using parton-hadron duality [13]. The wave function of the  $\rho$  meson then never enters explicitly. The only property that is used is that the  $\rho$  meson corresponds to the  $J^P = 1^-$  projection of ‘open’  $q\bar{q}$  production (with  $q = u, d$ ). The projection has the effect of curing the infrared divergence. The resulting cross section is

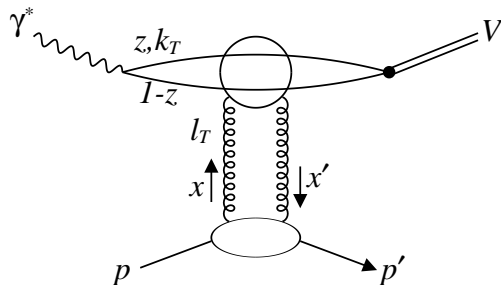


Figure 1: Schematic diagram for diffractive vector meson production at HERA,  $\gamma^*p \rightarrow Vp$ . The longitudinal fractions  $x$  and  $x'$  of the ingoing and outgoing proton momentum carried by the gluons are given by Eq. (10); the gluons have momenta  $\pm \ell_T$  transverse to the proton.  $z$  and  $1 - z$  are the longitudinal fractions of the photon momentum carried by the  $q$  and  $\bar{q}$ , and  $\pm \mathbf{k}_T$  are their momenta transverse to the photon. There are four possible couplings of the two gluons to the  $q$  and  $\bar{q}$ , represented by the upper circle.

then integrated over an appropriate interval  $\Delta M$  of the invariant mass of the  $q\bar{q}$  pair which covers the  $\rho$  resonance peak. As there are almost no other possibilities<sup>1</sup> for hadronization of the  $q\bar{q}$  pairs at  $M_{q\bar{q}} \simeq M_\rho$ , the procedure is expected to give a reasonable estimate of the cross section for  $\rho$  electroproduction. Indeed this perturbative framework [13] was found to describe

<sup>1</sup>We allow for  $\omega$  production by taking the ratio  $\omega : \rho$  to be 1:9.

the  $Q^2$  dependence of  $\rho$  electroproduction for  $Q^2 \gtrsim 5 \text{ GeV}^2$  for both longitudinally and transversely polarised  $\rho$  mesons, including the observed  $Q^2$  dependence of the  $\sigma_L/\sigma_T$  ratio. The  $Q^2$  behaviour of the amplitude is governed by the structure of the quark propagators and by the effective anomalous dimension  $\gamma$  of the gluon, defined by  $xg(x, K^2) \sim (K^2)^\gamma$ . In particular the naive expectation that  $\sigma_T = \sigma_L M^2/Q^2$  is modified to<sup>2</sup>

$$\frac{\sigma_L}{\sigma_T} = \frac{Q^2}{M^2} \left( \frac{\gamma}{\gamma + 1} \right)^2 \quad (1)$$

which, on account of the decrease of  $\gamma$  with increasing  $Q^2$ , is in good agreement with the observed  $\sigma_L/\sigma_T$  behaviour with  $Q^2$ .

The cross section for the diffractive electroproduction of vector mesons is proportional to the square of the off-diagonal or skewed gluon distribution. That is  $x \neq x'$  in Fig. 1, whereas for the conventional (diagonal) gluon we have  $x = x'$ . In fact the gluon distribution becomes more skewed as  $Q^2$  increases, and is more skewed for vector mesons of larger mass  $M$ . Skewed distributions were not included in our predictions of the  $Q^2$  behaviour of  $\rho$  electroproduction in Ref. [13]. When compared with subsequent precise HERA data [4], these predictions were found to fall off a bit too rapidly with increasing  $Q^2$ . We will see that the effect of using the skewed distribution, rather than the usual approximation of using the conventional (diagonal) gluon, will enhance the cross sections at the larger values of  $Q^2$  at which data exists. As was previously discussed [13], there are uncertainties in the normalization of the predictions of the diffractive cross sections, but much less in the predictions of the energy or  $Q^2$  dependence. Nevertheless, in order to use the  $Q^2$  dependence of the data to reveal the effects of the skewed distribution, we must include the  $Q^2$  dependence of other effects in our calculation. The (imaginary part of the) amplitude is calculated at  $t = 0$  and the cross section obtained by integrating  $d\sigma/dt \sim \exp(-bt)$  over  $t$ . We must therefore allow for the decrease of  $b$  with increasing  $Q^2$ . Second we must study the ambiguity in our estimates of the next-to-leading order (NLO) correction. In the perturbative region, we find that the  $Q^2$  variation of  $\rho$  electroproduction from these two sources is smaller than that due to the use of the skewed gluon distribution. Also we must, of course, include the contribution from the real part of the amplitude. When we compare the full QCD prediction with the  $Q^2$  behaviour of diffractive  $\rho$  and  $J/\psi$  production recently measured at HERA we find that the data are compatible with the characteristic enhancement arising from the skewed gluon.

We use perturbative QCD to derive the general formula for the cross section for diffractive vector meson production by first recalling the formula for diffractive production of a  $q\bar{q}$  system of mass  $M$ . For production from a transversely (longitudinally) polarised photon

$$\left. \frac{d^2\sigma^{T(L)}}{dM^2 dt} \right|_{t=0} = \frac{2\pi^2 e_q^2 \alpha}{3(Q^2 + M^2)^2} \int dz \left| B_{ii'}^{T(L)} \right|^2 \quad (2)$$

---

<sup>2</sup>Eq. (1) is an approximate result obtained assuming that, for each  $Q^2$ ,  $\gamma$  is constant throughout the integration over the quark loop. The full calculation can be found in Ref. [13]. See also the results discussed below.

where  $i = +, -$  and  $i' = +, -$  denote the helicity of the quark and antiquark. The helicity amplitudes are

$$\begin{aligned} \text{Im} B_{++}^T &= \frac{m I_L}{2\sqrt{z(1-z)}}, & B_{--}^T &= 0, \\ \text{Im} B_{+-}^T &= \frac{-zk_T I_T}{\sqrt{z(1-z)}}, & \text{Im} B_{-+}^T &= \frac{(1-z)k_T I_T}{\sqrt{z(1-z)}}, \end{aligned} \quad (3)$$

for a photon of helicity  $+1$ , whereas for a longitudinal photon we have

$$\begin{aligned} B_{++}^L &= B_{--}^L = 0, \\ \text{Im} B_{+-}^L &= -\text{Im} B_{-+}^L = \sqrt{\frac{z(1-z)Q^2}{2}} I_L. \end{aligned} \quad (4)$$

The variable  $z$  is the fraction of the photon's momentum carried by the quark,  $k_T$  is the transverse momentum of the quark relative to the photon,  $e_q$  is the charge (in units of  $e$ ) and  $m$  the mass of the quark;  $\alpha = 1/137$ . The mass  $M$  of the  $q\bar{q}$  system satisfies

$$M^2 = \frac{m^2 + k_T^2}{z(1-z)}. \quad (5)$$

The integrals over the transverse momentum  $\pm \ell_T$  of the exchanged gluons are [14, 13]

$$I_L(K^2) = \int \frac{d\ell_T^2}{\ell_T^4} \alpha_S(\ell_T^2) f(x, x', \ell_T^2) \left(1 - \frac{K^2}{K_\ell^2}\right), \quad (6)$$

$$I_T(K^2) = \frac{K^2}{2} \int \frac{d\ell_T^2}{\ell_T^4} \alpha_S(\ell_T^2) f(x, x', \ell_T^2) \left[\frac{1}{K^2} - \frac{1}{2k_T^2} + \frac{K^2 - 2k_T^2 + \ell_T^2}{2k_T^2 K_\ell^2}\right], \quad (7)$$

where

$$K^2 = z(1-z)Q^2 + k_T^2 + m^2, \quad (8)$$

$$K_\ell^2 = \sqrt{(K^2 + \ell_T^2)^2 - 4k_T^2 \ell_T^2}. \quad (9)$$

The function  $f(x, x', \ell_T^2)$  is the skewed unintegrated gluon distribution describing the lower part of Fig. 1. The momentum fractions carried by the exchanged gluons satisfy [15]

$$\left(x \simeq \frac{Q^2 + M^2}{W^2 + Q^2}\right) \gg \left(x' \simeq \frac{\ell_T^2}{W^2 + Q^2}\right) \quad (10)$$

where  $W$  is the  $\gamma^* p$  centre-of-mass energy.

In the strict leading  $\log(1/x)$  approximation, it is enough to use the diagonal unintegrated distribution, as at each splitting we keep just the leading  $\log(1/x)$  terms and neglect the corrections due to  $x' \ll x$ . In this limit

$$f(x, x', \ell_T^2) = f(x, \ell_T^2) = \left. \frac{\partial(xg(x, \mu^2))}{\partial \ln \mu^2} \right|_{\mu^2=\ell_T^2} \quad (11)$$

and there is no difference between the diagonal and skewed distributions [16]. This is the approximation which is conventionally used.

Here we wish to take into account the skewed effect, but first we must extend the definition of the unintegrated gluon, (11), beyond the leading  $\log(1/x)$  approximation. Indeed it is easy to see that (11) can only be true for sufficiently small  $x$ . If  $x$  increases then  $f$  calculated from (11) would soon become negative due to the (negative) virtual contribution in the DGLAP evolution. It was shown in Ref. [17] that the virtual corrections may be resummed via the Sudakov form factor and that the number of gluons with transverse momentum  $\ell_T$  is

$$f(x, \ell_T^2) = \left. \frac{\partial[xg(x, q_0^2) T(q_0^2, \mu^2)]}{\partial \ln q_0^2} \right|_{q_0^2=\ell_T^2}, \quad (12)$$

where in the double log approximation (DLA)

$$T(q_0^2, \mu^2) = \exp \left[ \frac{-C_A \alpha_S(\mu^2)}{4\pi} \ln^2 \frac{\mu^2}{q_0^2} \right], \quad (13)$$

with scale  $\mu^2 \sim (Q^2 + M^2)/4$ .  $T$  is a survival probability. It is the probability that the parent gluon does not emit gluons in the interval  $q_0^2 < q_T^2 < \mu^2$ . From the formal point of view, the  $T$  factor may be regarded as a next-to-leading order correction since the main contributions to the integrals (6) and (7) come from the region<sup>3</sup>  $\ell_T^2 \lesssim \mu^2$ . In general we find that the inclusion of  $T$  has a small effect, essentially only ensuring the positivity of  $f$  for  $\Upsilon$  production which samples values of  $x$  as large as  $x \sim 0.05$ .

The main effect of using the skewed (or off-diagonal) gluon distribution comes, within leading  $\ln Q^2$  kinematics, from the region where  $x' \ll x$ , see (10). In this region the skewed gluon distribution  $H_g(x, x')$  (integrated over  $\ell_T$ ) is larger than the conventional diagonal distribution  $H_g(x, x) = xg(x)$ . For small  $x$ , which is appropriate for vector meson production at HERA, the enhancement is generated entirely by off-diagonal evolution. Moreover the ratio

$$R_g = \frac{H_g(x, x' \ll x)}{H_g(x, x)} \quad (14)$$

---

<sup>3</sup>If  $\ell_T > \mu$  then we set  $T = 1$  in (12), consistent with the DLA. It may occasionally happen (at the edge of phase space) that the inclusion of the  $T$  factor in the DLA is not enough to ensure the positivity of  $f(x, \ell_T^2)$ , whereas the exact form of the  $T$  factor would guarantee that  $f > 0$ . Therefore we set  $f = 0$  if it should happen that (12) is negative.

can be determined unambiguously in terms of the known diagonal distribution [18]. It was shown that the enhancement  $R_g$  depends on the effective power  $\lambda(Q^2)$  of the small  $x$  behaviour of the gluon  $xg \sim x^{-\lambda}$ . The result is [18]

$$R_g = \frac{2^{2\lambda+3}}{\sqrt{\pi}} \frac{\Gamma\left(\lambda + \frac{5}{2}\right)}{\Gamma(\lambda + 4)}. \quad (15)$$

Note that the off-diagonal enhancement enters at leading order (in  $\ln Q^2$ ) and increases with  $Q^2$  (since  $\lambda$  increases with  $Q^2$ ). Here we allow for the off-diagonal effect by multiplying the amplitudes (3) and (4), calculated<sup>4</sup> with diagonal gluons in (6) and (7), by the factor  $R_g$ . We determine the effective power for each component amplitude separately, that is

$$\lambda = \frac{\partial \log B_{ii'}}{\partial \log(1/x)}. \quad (16)$$

The full NLO corrections for the diffractive process are not known yet, and so we approximate them by a  $\mathcal{K}$  factor [14, 13]. Following [14], the main ( $\pi^2$  enhanced) part of the  $\mathcal{K}$  factor is of the order of  $(\pi^2 C_F \alpha_S / \pi)$ , where  $C_F = 4/3$ . It comes from the  $i\pi$  terms in the double logarithmic Sudakov form factor  $\exp[-C_F(\alpha_S/4\pi) \ln^2(-M^2)]$  where  $\ln(-M^2) = \ln M^2 + i\pi$ . Thus we multiply the amplitudes by the factor [14]

$$\mathcal{K} = \exp(\pi C_F \alpha_S / 2). \quad (17)$$

But we still have the ambiguity of the choice of the scale of  $\alpha_S$ . We show results for two choices of scale:  $\mu^2 = K^2$  and our default value  $\mu^2 = 2K^2$ , where  $K^2$  is given by (8).

To include the contribution from the real part of the amplitude we use the signature factor

$$\mathcal{S}^{(+)} = i + \tan(\pi\lambda/2) \quad (18)$$

for positive signature exchange. This is a simple way of implementing the dispersion relation result. It gives

$$\text{Re} B_{ii'} = \tan(\pi\lambda/2) \text{Im} B_{ii'}, \quad (19)$$

where  $\lambda$  is given by (16). The inclusion of the real part enhances the cross section of  $\rho$  production by 14 to 19% in the range where we compare to data,  $J/\psi$  production by 18 to 25%, and  $\Upsilon$  by about 30%, where the bigger effect always occurs at higher  $Q^2$ .

So far we have calculated the cross section  $d^2\sigma/dM^2 dt$  for diffractive  $q\bar{q}$  production at  $t = 0$ . To determine  $d\sigma/dM^2$  we integrate the form  $\exp(-bt)$  over  $t$ , with [19]

$$b(Q^2) = \frac{4}{(\langle t \rangle + 0.71 \text{ GeV}^2)} + \frac{2}{Q^2 + M^2 + \langle t \rangle} + 2\alpha'_P \ln \left( \frac{W^2 M^2}{(Q^2 + M^2)^2} \right), \quad (20)$$

---

<sup>4</sup>In the infrared region  $\ell_T^2 < \ell_0^2$  we use the “linear” approximation  $\alpha_S(\ell_T^2)g(x, \ell_T^2) = (\ell_T^2/\ell_0^2)\alpha_S(\ell_0^2)g(x, \ell_0^2)$  as described in [14]. This linear approximation is reasonable since (i) it corresponds to a constant gluon-proton cross section at small scales  $\ell_T < \ell_0$  and (ii) it matches well to the scale dependence of the phenomenological gluon distribution at low  $\ell_T$ . We have checked that our results are stable to reasonable variations of  $\ell_0^2$  about our default value of 1.5 GeV<sup>2</sup>.

where  $\langle t \rangle$  is the average value of  $t$ . (Here we set  $\langle t \rangle = 0$ .) This form, with  $\alpha'_{\mathbb{P}} = 0.15 \text{ GeV}^{-2}$ , successfully reproduces the  $t$  behaviour of diffractive  $\rho$  meson leptonproduction data as a function of  $Q^2$  and  $M^2 \simeq M_V^2$ . It is motivated by the additive quark model, together with a form factor given by  $F_V(t) = M^2/(M^2 - t)$ , see also [20]. We also use the phenomenological expression (20) for diffractive  $J/\psi$  production even though the measured slopes appear, at present, to be about  $2 \text{ GeV}^{-2}$  or 30% less. Using the observed values of  $b$  would lead to an overall increase in the  $J/\psi$  cross section of about 30%, well within the present uncertainties in the theoretical normalization.

To determine the cross section for  $\gamma^*p \rightarrow Vp$  from that for diffractive  $q\bar{q}$  production, we project out the  $J^P = 1^-$  state in the  $q\bar{q}$  rest frame. However the helicity amplitudes  $B_{ii'}$  are defined in the target proton rest frame, and helicity is not conserved by Lorentz transformations for the heavy quark states. So to obtain the helicity amplitudes  $A_{jj'}$  in the  $q\bar{q}$  rest frame for  $V = J/\psi$  and  $\Upsilon$ , we must perform a Lorentz boost and use

$$A_{jj'} = \sum_{i,i'} c_{ij} c_{j'i'} B_{ii'}, \quad (21)$$

where the known coefficients  $c_{ij}$  are given in Ref. [21]. Finally we integrate the cross section  $d\sigma/dM^2$  for  $J = 1^- q\bar{q}$  production over an appropriate interval  $\Delta M^2$  covering the vector meson resonance. Clearly this, together with the  $\mathcal{K}$  factor of (17), introduces an overall normalization uncertainty. However here we are interested in the  $Q^2$  dependence of  $\sigma(\gamma^*p \rightarrow Vp)$  and the properties of the ratio  $\sigma_L/\sigma_T$ , rather than the normalization.

The QCD predictions for  $\rho$ ,  $J/\psi$  and  $\Upsilon$  production<sup>5</sup> are compared with HERA data in Figs. 2–4. Fig. 2 shows the predictions obtained from using three different recent gluon distributions: MRST [22], CTEQ [23] and KMS [24]. All fit the  $F_2$  structure function data well. The first two are obtained from conventional NLO DGLAP analyses, while the KMS analysis is in terms of an unintegrated gluon distribution which satisfies a unified BFKL/DGLAP equation with subleading  $\ln(1/x)$  contributions. In each case the scale  $\mu^2$  in  $\alpha_S$  of the  $\mathcal{K}$  factor is taken to be  $2K^2$ . The lower continuous curves in Fig. 2 correspond to the ‘default’ prediction obtained using MRST99 partons. In both plots the upper continuous curve corresponds to taking  $\mu^2 = K^2$ . The dashed curve is the default prediction using the diagonal gluon, and so comparison with the lower continuous curve shows the enhancement due to off-diagonal effects. At the larger values of  $Q^2$  the enhancement is about 55% for  $\rho$  production and 70% for  $J/\psi$  production.

Our approach is infrared finite. However there are non-negligible contributions from the region of low gluon transverse momenta  $\ell_T < \ell_0$ . Fortunately the predictions based on conventional DGLAP partons (MRST, CTEQ) are rather insensitive to the choice of the value of  $\ell_0$ . Nevertheless to check the infrared sensitivity of the predictions we also use a gluon obtained

---

<sup>5</sup>The  $J/\psi$  production amplitudes were calculated for a charm quark mass  $m_c = 1.4 \text{ GeV}$ , whereas for  $\Upsilon$  production we take the  $b$  quark mass  $m_b = 4.6 \text{ GeV}$ .

from a unified BFKL/DGLAP analysis of the deep inelastic data [24].<sup>6</sup> We would expect some difference since the latter (Reggeised) gluon embodies a higher twist component originating from the BFKL evolution, which may be important at low scales. Indeed we see from the dotted curves in Fig. 2 that the cross sections are considerably larger than the DGLAP-based predictions particularly at low values of  $Q^2$ . This demonstrates the need to better understand the role of higher twist (and power) corrections in parton analyses. Diffractive vector meson production is clearly a good process in which to further investigate these effects.

In the parton-hadron duality approach we have a common mechanism for the description of all vector meson production processes,  $\gamma^*p \rightarrow Vp$ , governed by the average hard scale  $\langle K^2 \rangle$ , where

$$K^2 = z(1-z)(Q^2 + M_V^2). \quad (22)$$

Therefore it is informative to plot all the observed cross sections, in a given  $W$  domain, as a function of  $Q^2 + M_V^2$  on the same plot, after allowing for the different photon-quark couplings  $e_q$  (that is  $\rho : J/\psi : \Upsilon = 9 : 8 : 2$ ) and the different energies  $W$  of the data. The result is compared with the  $\rho$  prediction in Fig. 3. The fact that the measured cross sections approximately lie on a common curve, demonstrates the universality inherent in the perturbative QCD description. Some departure from universality may arise from the different measured  $t$  slopes, from the flavour symmetry breaking of the  $q\bar{q} \rightarrow V$  transition<sup>7</sup>, and from comparing data with different average  $W$  values.

Figs. 4, 5 show the QCD predictions for  $\sigma_L/\sigma_T$ . The upper (lower) plot of Fig. 4 compare the ratio for  $\rho$  ( $J/\psi$ ) electroproduction with the recent HERA data as a function of  $Q^2$  at fixed energy  $W = 75$  GeV ( $W = 90$  GeV), whereas Fig. 5 shows the  $W$  dependence for fixed values of  $Q^2$  for both  $\rho$  and  $J/\psi$  production. Recall that in Ref. [11] it was pointed out that only  $\sigma_L$  is calculable in perturbative QCD; the calculation of  $\sigma_T(\rho)$  using the leading twist  $\rho$  meson wave function is infrared divergent. We must therefore explain how the  $\sigma_L/\sigma_T$  curves can be obtained? In the parton-hadron duality approach, with the  $J^P = 1^-$  projection of the  $q\bar{q}$  system, the integral over the quark  $k_T$  is of logarithmic form [13] (like in a usual DIS amplitude). So the corresponding Feynman graphs have (at leading order) a pure ladder structure with strong  $k_T$  ordering along the ladder. The factorization theorem is therefore valid for  $\sigma_T$ , as well as  $\sigma_L$ . After convolution with the gluon distribution, the logarithmic behaviour effectively enhances the transverse amplitude by a factor  $1/\gamma$ , so  $\sigma_T \sim 1/\gamma^2$  as in (1). The decrease of  $\gamma$  with increasing  $Q^2$  masks the naive  $Q^2/M^2$  expectation for the  $Q^2$  behaviour of  $\sigma_L/\sigma_T$ .

---

<sup>6</sup>In [24] the value of the unintegrated gluon is determined down to  $\ell_T = k_0 = 1$  GeV. Below  $k_0$  we use the linear approximation as was described in footnote 4 above, with  $xg(x, k_0) = 1.57(1-x)^{2.5}$ .

<sup>7</sup>In the non-relativistic approximation the  $q\bar{q} \rightarrow V$  vertices are proportional to the meson wave functions evaluated at the origin, which may differ according to the mass of the meson. In our approach this is replaced by the different  $z$  intervals sampled by the relativistic  $\rho$  system as compared to the more non-relativistic  $J/\psi$  and  $\Upsilon$  systems and by possible different choices of the mass interval  $\Delta M$  covering the resonance peaks. Here the same value  $\Delta M = 200$  MeV was used for  $\rho$  and  $J/\psi$  production. For the  $\Upsilon$  the interval  $M = 8.9 \dots 10.9$  GeV was chosen to predict  $\Upsilon(1S, 2S, 3S)$  production in accordance with the experimental analysis [7], and the resulting cross sections were divided by 1.7 to get the predictions for  $\Upsilon(1S)$ , see [21].



It is interesting to compare the predictions for the  $W$  behaviour of  $\sigma_L/\sigma_T$  for  $J/\psi$  production with those for  $\rho$  production, shown respectively by the dashed and continuous curves in Fig. 5. For  $\rho$  production we are in a relativistic  $q\bar{q}$  situation where  $z$  covers an extensive part of the (0,1) interval allowing the  $1/\gamma$  behaviour to develop. The growth of  $\sigma_L/\sigma_T$  with  $W$  reflects the rise of  $\gamma$  with  $1/x$ . On the other hand  $J/\psi$  production is nearer the non-relativistic limit where  $z = 1/2$  and  $\sigma_L/\sigma_T = Q^2/M^2$  apply, and hence the ratio  $\sigma_L/\sigma_T$  is almost independent of  $W$ .

To gain physical insight we have discussed the results in terms of an effective gluon anomalous dimension  $\gamma$  and the simplified formula (1). In the actual computations we use, of course, the explicit unintegrated (skewed) gluon distributions and perform the full integrations over  $k_T$  and  $\ell_T$ , or related variables.

In summary we have shown that a perturbative QCD parton-hadron duality approach is able to describe all the main features of the  $\sigma_L$ , and even the  $\sigma_T$ , data for diffractive vector meson production  $\gamma^*p \rightarrow Vp$ , *provided* that there is a sufficiently hard scale (that is provided  $Q^2 + M^2$  is greater than about 5 GeV<sup>2</sup>). We emphasize that the approach is infrared convergent. There are non-negligible contributions at low gluon transverse momentum  $\ell_T$ , but the perturbative gluon form matches well on to the linear  $\ell_T^2$  form for  $\ell_T < \ell_0$  making the predictions rather insensitive to the choice of  $\ell_0$ . The effects of using skewed gluons are fully included in the QCD calculations. The skewed distribution is completely determined by the conventional (diagonal) gluon distribution, and is found to enhance the  $\rho$  and  $J/\psi$  cross sections by about 55% and 70% respectively at the largest observed values of  $Q^2$ . For  $\rho$  production the use of the skewed gluon distribution predicts a flatter  $Q^2$  dependence, compatible with the recent data, see Fig. 2. We conclude that the data for diffractive vector meson production processes at HERA offer a particularly sensitive probe of the properties of the gluon distribution of the proton. The  $M$ ,  $Q^2$ ,  $t$  dependences and the spin properties can be measured with increased precision and all constrain the behaviour of the gluon.

## Acknowledgements

One of us (MGR) thanks the Royal Society and the Russian Fund for Fundamental Research (98-02-17629) for support. Part of this work was carried out while TT was at DESY. The work was also supported by the EU Framework TMR programme, contract FMRX-CT98-0194. We thank Anna Stasto for valuable information.

# References

- [1] H1 collaboration, S. Aid et al., Nucl. Phys. **B468** (1996) 3.
- [2] H1 collaboration, S. Aid et al., Nucl. Phys. **B472** (1996) 3.
- [3] H1 collaboration, Conference Paper 574, B. Naroska, contributed to the 29th Intern. Conf. on High-Energy Physics (ICHEP98), Vancouver, Canada (1998).
- [4] H1 collaboration, C. Adloff et al., DESY-99-010 and hep-ex/9902019, Eur. Phys. J. **C** (in press).
- [5] H1 collaboration, C. Adloff et al., Eur. Phys. J. **C10** (1999) 373.
- [6] ZEUS collaboration, J. Breitweg et al., Z. Phys. **C75** (1997) 215.
- [7] ZEUS collaboration, J. Breitweg et al., Phys. Lett. **B437** (1998) 432.
- [8] ZEUS collaboration, J. Breitweg et al., Eur. Phys. J. **C6** (1999) 603.
- [9] ZEUS collaboration, J. Breitweg et al., DESY-99-102 and hep-ex/9908026.
- [10] A. Donnachie and P.V. Landshoff, Phys. Lett. **B185** (1987) 403; Erratum-ibid. **B198** (1987) 590; Nucl. Phys. **B311** (1989) 509; Phys. Lett. **B437** (1998) 408.
- [11] S.J. Brodsky et al., Phys. Rev. **D50** (1994) 3134.
- [12] B.Z. Kopeliovich et al., Phys. Lett. **B309** (1993) 179.  
J. Nemchik, N.N. Nikolaev, B.G. Zakharov, Phys. Lett. **B341** (1994) 228.  
L. Frankfurt, W. Koepf and M. Strikman, Phys. Rev. **D54** (1996) 3194.  
J. Nemchik et al., Z. Phys. **C75** (1997) 71; Phys. Lett. **B374** (1996) 199.  
N.N. Nikolaev and B.G. Zakharov, hep-ph/9706343, talk given at the *5th International Workshop on Deep Inelastic Scattering and QCD (DIS 97)*, Chicago, IL, USA, April 1997.  
D. Schildknecht, G.A. Schuler and B. Surrow, Phys. Lett. **B449** (1999) 328.  
I. Royen and J.R. Cudell, Nucl. Phys. **B545** (1999) 505.
- [13] A.D. Martin, M.G. Ryskin and T. Teubner, Phys. Rev. **D55** (1997) 4329.
- [14] E.M. Levin, A.D. Martin, M.G. Ryskin and T. Teubner, Z. Phys. **C74** (1997) 671.
- [15] A.D. Martin and M.G. Ryskin, Phys. Rev. **D57** (1998) 6692.
- [16] J. Bartels and M. Loewe, Z. Phys. **C12** (1982) 263.
- [17] Yu.L. Dokshitzer, D.I. Diakonov and S.I. Troian, Phys. Rep. **58** (1980) 269.
- [18] A.G. Shuvaev, K.J. Golec-Biernat, A.D. Martin and M.G. Ryskin, Phys. Rev. **D60** (1999) 014015.

- [19] M.G. Ryskin, Yu.M. Shabelski and A.G. Shuvaev, Phys. Lett. **B446** (1999) 48.
- [20] L.P.A. Haakman, A. Kaidalov and J.H. Koch, Phys. Lett. **B365** (1996) 441.
- [21] A.D. Martin, M.G. Ryskin and T. Teubner, Phys. Lett. **B454** (1999) 339.
- [22] A.D. Martin, R.G. Roberts, W.J. Stirling and R.S. Thorne, Eur. Phys. J. **C4** (1998) 463.
- [23] CTEQ collaboration, H.L. Lai et al., MSU-HEP-903100 and hep-ph/9903282.
- [24] J. Kwiecinski, A.D. Martin and A.M. Stasto, Phys. Rev. **D56** (1997) 3991.

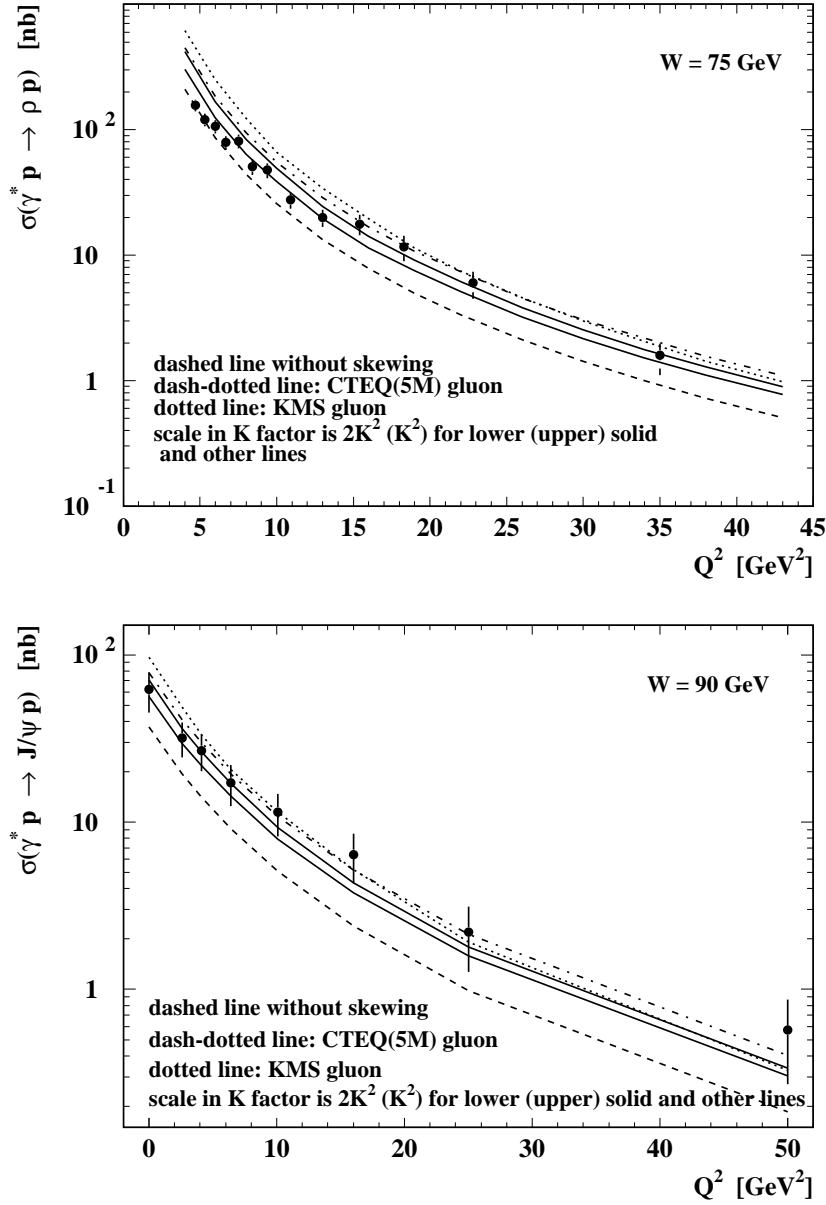


Figure 2: The QCD predictions for the  $Q^2$  dependence of the cross sections for  $\gamma^* p \rightarrow \rho p$  (upper plot,  $W = 75 \text{ GeV}$ ) and  $\gamma^* p \rightarrow J/\psi p$  (lower plot,  $W = 90 \text{ GeV}$ ) compared with the HERA data [4, 5]. The continuous curves are obtained using the MRST(99) gluon [22]. For the lower curve the default value  $2K^2$  is chosen for the scale of  $\alpha_s$  in the  $\mathcal{K}$  factor, whereas for the upper curve the scale  $K^2$  was used. The dash-dotted (dotted) curves show the results if the CTEQ(5M) [23] (KMS [24]) gluon are used. The dashed curves show our results using the MRST(99) gluon and default parameters but without the effect of skewing. All predictions contain contributions from the real part of the amplitude as discussed in the text. The data point for  $J/\psi$  photoproduction in the lower plot is interpolated between H1 data for different values of  $W$  [2] and agrees well with the ZEUS result [6].

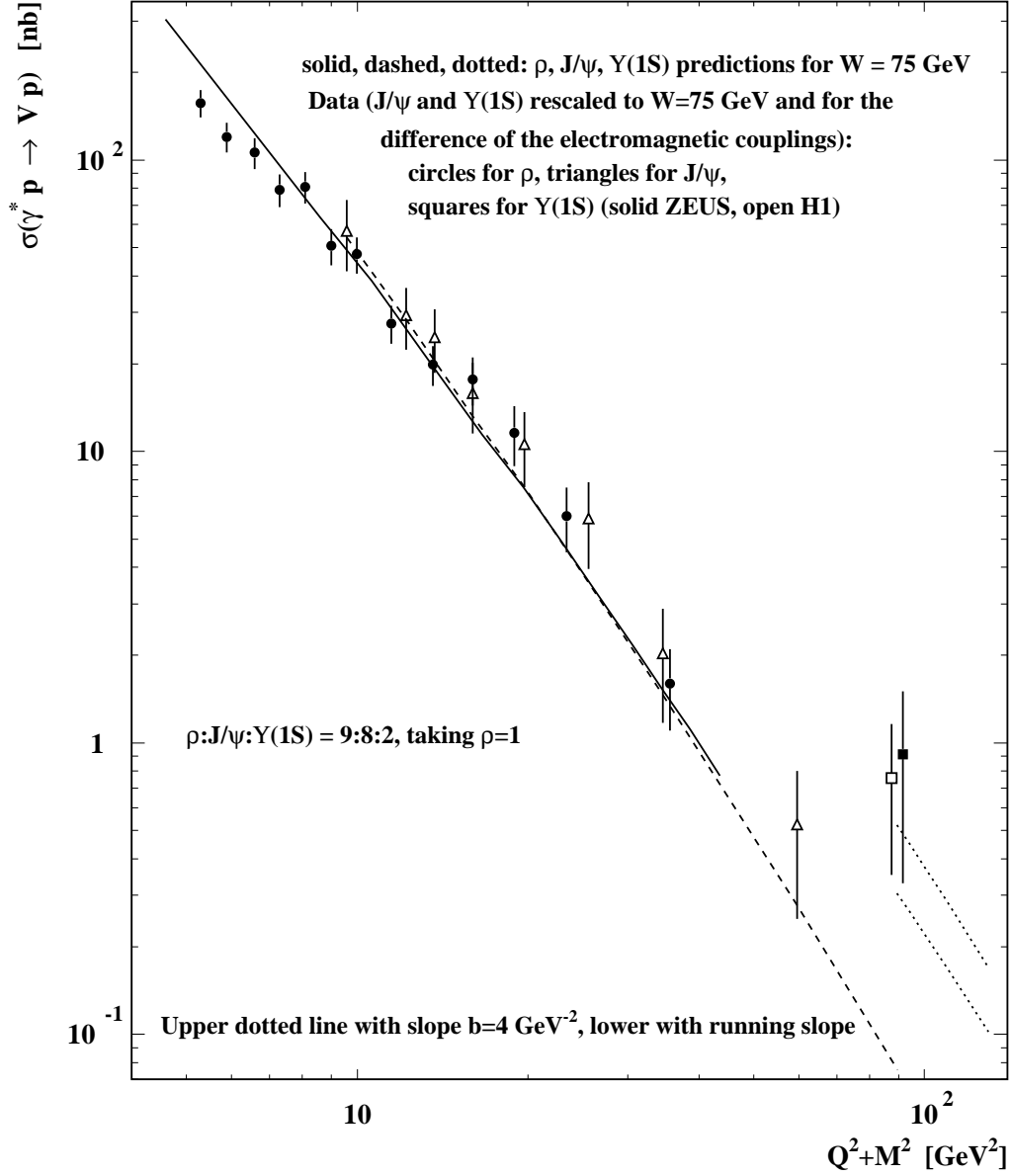


Figure 3: The data [4, 5, 2, 3, 7] for the  $\gamma^* p \rightarrow V p$  cross sections with  $V = \rho$  (circles),  $J/\psi$  (triangles) and  $\Upsilon(1S)$  (squares: solid ZEUS, open H1, both slightly displaced from  $Q^2 = 0$  for readability) plotted versus  $Q^2 + M_V^2$ . The QCD predictions (with standard parameters as described in the text) are shown for comparison as continuous, dashed and dotted lines, respectively. The  $J/\psi$  and  $\Upsilon$  data (and errors) are corrected for (i) the different photon-quark couplings by multiplying the  $J/\psi$  and  $\Upsilon$  measurements by 9/8 and 9/2 respectively, (ii) the different  $W$  values according to the QCD predicted energy behaviour  $\sigma(J/\psi) \sim W^{1.1}$  (in agreement with the experimental measurements from [5]) and  $\sigma(\Upsilon) \sim W^{1.3}$ . The upper dotted curve is obtained using a fixed slope parameter  $b = 4 \text{ GeV}^{-2}$ , whereas the lower curve contains the slope as given in Eq. (20).

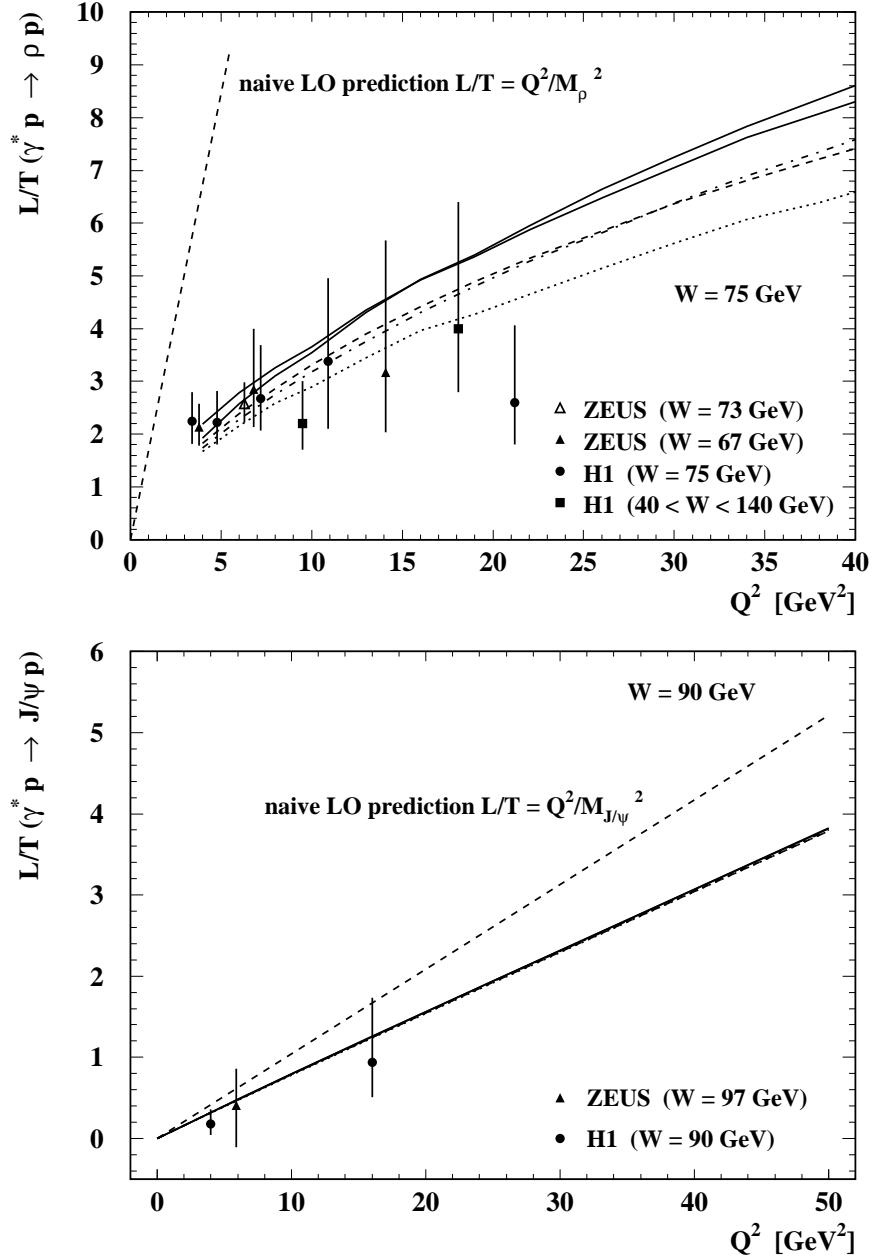


Figure 4: The upper plot shows the QCD predictions for the  $Q^2$  dependence of  $\sigma_L/\sigma_T$  for  $\rho$  electroproduction (at  $W = 75$  GeV) compared with HERA data [4, 1, 8, 9], partially at slightly different (average) values of  $W$  as indicated on the plot. The ZEUS measurement displayed by the open triangle is the one obtained by relaxing the  $s$ -channel helicity conservation condition, see [9]. The different linestyles for the different gluons are chosen as in Fig. 2. Here the steeper continuous curve corresponds to the standard choice of  $2K^2$  as scale of  $\alpha_S$  in the  $\mathcal{K}$  factor, the less steeper one to  $K^2$ . Also displayed is the naive expectation  $\sigma_L/\sigma_T = Q^2/M_\rho^2$  (steep dashed line). The lower plot shows  $\sigma_L/\sigma_T$  for  $J/\psi$  production (at  $W = 90$  GeV) compared to data from [5, 8].

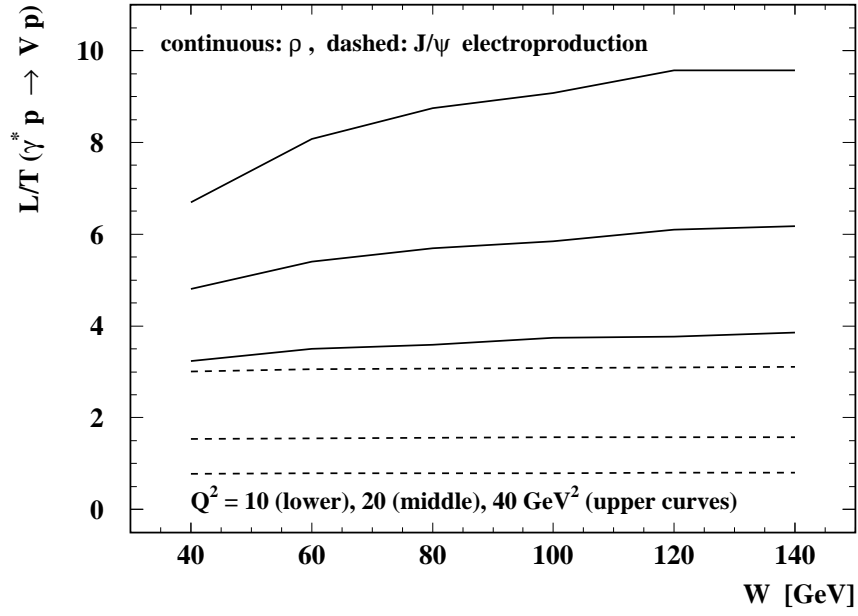


Figure 5: The  $W$  behaviour of  $\sigma_L/\sigma_T$  for fixed values of  $Q^2$  for both  $\rho$  electroproduction (continuous curves) and  $J/\psi$  electroproduction (dashed curves), obtained with our default parameters and the MRST(99) gluon.